Electronic and Optical Properties of $Feni_3$ Alloy

Yamina Benkrima[1,*], Soufiane Benhamida[2], Djamel Belfennache[3], Radhia Yekhlef[3,4]

[1]Department of Exact Sciences, ENS Ouargla, Algeria.

[2]Laboratory of Radiation, Plasma and Surface Physics (LRPPS), Faculty of Mathematics and Material Sciences, Kasdi Merbah Ouargla University, Route de Ghardaia, BP n°511, Ouargla 30000, Algeria.

[3]Research Center in Industrial Technologies CRTI, P.O. Box 64, Cheraga, 16014 Algiers, Algeria.

[4]Laboratory of Electrochemistry, Molecular Engineering and Redox Catalysis (LEIMCR) Department of Engineering Process, Faculty of Technology, Ferhat Abbas University Setif-1, Setif 19000, Algeria.

*Correspondence Author-mail: b-amina1@hotmail.fr

Received: 05/2023, Published: 06/2023

Abstract:

The ab initio pseudopotential method is based on Density Functional Theory (DFT), where we use the generalized gradient approximation (GGA) according to the scheme described by Perdew-Burke-Ernzerhof (PBE). The method is embodied using the Siesta program, which works to study the structural, and optical properties of the nickel iron alloy (Fe-Ni) which crystallizesas ($FeNi_3$). In fact, this method is one of the best methods for predicting the crystal structure and alloy propertiesof $FeNi_3$. In fact, the calculated structural parameters for this compound are very consistent with the available theoretical and experimental data, so these results can be considered as a good prediction. The lattice constants was calculated at zero pressure value, to be consistent with previous theoretical and experimental results. All the calculated properties, such as the absorption coefficient, reflectivity and optical conductivity show that the alloy has distinctive values. This is what makes us think of using it for specific applications in specific fields.

Keywords: DFT, $FeNi_3$, Absorption coefficient, Reflectivity coefficient, Optical conductivity

Tob Regul Sci. ™ 2023;9(1): 2563-2570

DOI: doi.org/10.18001/TRS.9.1.177

1. Introduction

Fe-Ni system, and in particular, $FeNi_3$ (Permalloy criterion), has been studied for a long time over a wide range of electromagnetic microwave, magnetic recording devices ...ext [1,2], it is also

used in many advanced sensitive applications, due to its high magnetic permeability, low strength, close to zero magnetic stenosis, and anisotropic magnetic resistance, depending on the surrounding conditions. On the other hand, if we shed light on the mechanical properties, we find that $FeNi_3$ is an alloy with low strength and corrosion resistance at the same time, which makes the alloy with wide uses. Iron-nickel alloys, as traditional soft magnetic materials, have received great attention because of their high saturation (MS) magnetization, high permeability, and high Curie temperature, while their energy loss is low. Thanks to these features, they have been widely used in absorbing electromagnetic waves, magnetic sensors, magnetic recording heads, and even medicines [3].Among the studies previously done on fcc Fe-Ni alloys, those with a concentration of 65% Fe showed almost no thermal expansion at room temperature [4]. It was observed that the other metallic systems also show the same unique invar behavior. Numerous theoretical and experimental studies have been conducted on iron-based alloys such as Fe_3Ni, Fe_3Pt, and Fe_3Pd [5-8]. However, among these alloys, Fe-Ni alloys can be considered to be among the oldest known materials, the most important from a modern technological point of view, and the best even from an experimental point of view [5].

Fe-Ni alloys have attracted researchers because of their excellent Electronic,thermal, magnetic and optical properties [9]. Numerous experimental research studies have been conducted on both iron and nickel alloys, using neutron and Mossauer experiments, as well as X-ray diffraction [10-12]. The Fe-Ni system has been thermodynamically evaluated to define the Gibbs energy of Fe-Ni stable and metastable phases: liquid, A1 and related fcc-based ordered phases (L12 Fe_3Ni, L10 FeNi and L12 $FeNi_3$), A2 and related bcc-based ordered phases (D03 Fe_3Ni, B2 and B32 FeNi, D03 $FeNi_3$) [13].The lattice dynamic, thermodynamic and magnetic properties of some of them have been studied for different important phases of the Fe-Ni alloy such as L12 $FeNi_3$, taenite L10 FeNi and L12Fe_3Ni using the density functional theory method [14]. Many researchers have studied the structural constants, elastic, electronic and magnetic properties of three Fe-Ni binary metals ($FeNi_3$, FeNi and Fe_3Ni) under pressure change using first principle DFT [15,16].

This work is based on the structural, electronic, magnetic and optical of $FeNi_3$ alloy properties, and the results are discussed in the framework of the theory of density function DFT [17]. They are summarized as follows. First, Section 2 describes the method and the relevant computational parameters used in the calculations. Then, in Section 3.2, the computed results of the electronic properties of these oxides in terms of band structure and density of states (DOS) are discussed, with an analysis of the optical properties added in Section 3.3. Finally, Section 4 provides a summary of the study.

2. Theoretical method of calculation

The electronic structure calculations of $FeNi_3$ alloy were performed using the density functional theory (DFT) [17], as implemented in the SIESTA program [18]. It is noted that this code uses norm-conserving Troullier-Martins nonlocal pseudopotentials, and at the same time, as the

researchers note, shares flexible basis sets of localized Gaussian type atomic orbitals. The exchange correlation energy was evaluated using the generalized gradient approximation (GGA) parameterized by Perdew, Burke, and Ernserh (PBE) [19]. The self-consistent field (SCF) calculations were carried out with convergence criterion of 10^{-4}a.u. for the total energy; we used a double ζ polarized (DZP) basis with polarization function for Fe and Ni atoms. For an energy shift parameter of 80 meV, the variation density was intended in a regular real-space grid with a cut-off energy of 350 eV. The simulated alloy was positioned in a big cubic supercell with a parameter. To sample the Brillouin zone, only a single k-point centered at Γ was used because of the extended size of the super cell. The conjugated gradient method within Hellmann-Feynman forces was used and all the forces after structural relaxation were less than 10^{-3}eV/Å. Actually, 0.05 Å was the value of the maximum tolerance for ion displacement in the atoms of $FeNi_3$ alloy.

3. Results and discussion

3.1. The optimized structures

Our calculations in this work were based on the siesta program which was used to find the initial cell constants for the $FeNi_3$ alloy. In this regard, the results have been compared with the experiment data and the previous independent works; we present in Table 1 the structural parameters of the initial $FeNi_3$ cell. We obtained that the cell dimension of the $FeNi_3$ crystal (see Figure 1) is similar to what was previously reported, as it was characterized by a cell character length of 3.528 Å and a cell volume of 43.88 Å. What is recorded in Table 1 is very close to the previous theoretical and applied works.

Table 1. Structural parameters of the optimized alloy $FeNi_3$ and compared with theoretical and experimental result.

work	a (Å)	V (Å)
Our work	3.528	43.88
Theor [20]	3.548	44.662
Theor [21]	3.50	/
Exp [21]	3.55	/

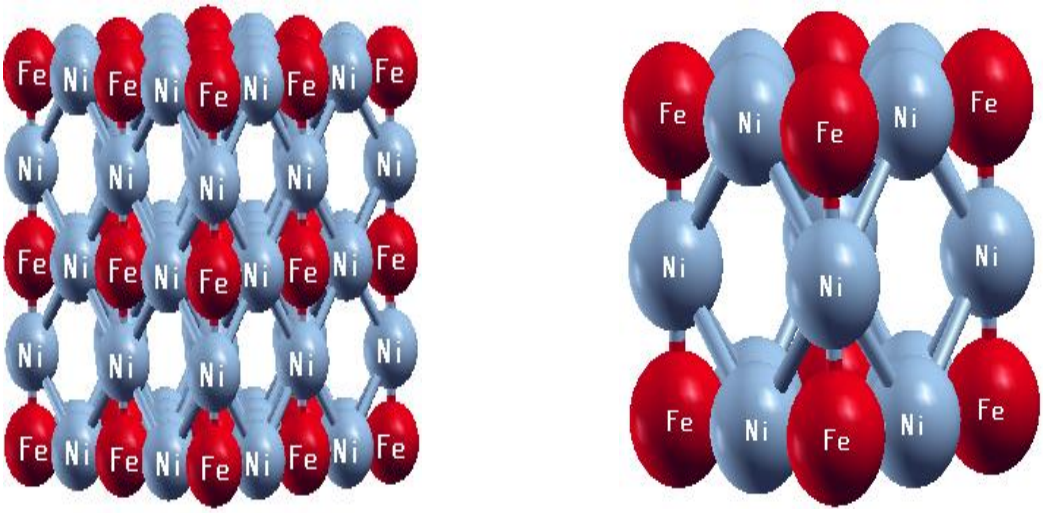

(a) (b)

Fig. 1. Optimized of $FeNi_3$ alloy, (a) unit cell, (b) supercell (2x2x2) visualized by SIESTA package.

3.2. Optical Properties

The importance of studying the optical properties of materials lies in obtaining information about the values of the optical constants of the material in a wide range of wavelengths, as this information is used in the design and manufacture of optical pieces and optical pulses.

3.2.1. Absorption coefficient

The absorption coefficient depends on the energy of the incident photons and the properties of the conductors. Where the nature of the electronic transitions occurring can be known from the values of the absorption coefficient, its equation is given in the form:

$$\alpha = \frac{4\pi k}{\lambda} \quad (1)$$

Where: α is absorption coefficient, k is the coefficient of extinction and λ is wave length (cm). Figure 2 shows the absorption coefficient of the $FeNi_3$ alloy.

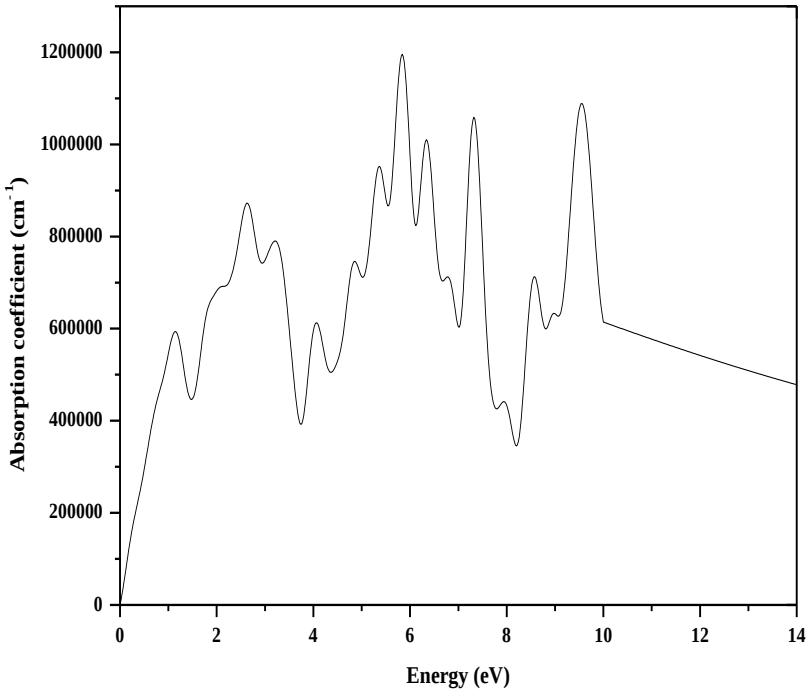

Fig. 2. Absorption coefficientof $FeNi_3$alloy.

Figure.2 shows the change in the absorption coefficient as a function of the energy of the incident photon on the $FeNi_3$ alloy. From the figure it is clear that the absorption increases gradually with the increase in the energy of photons, in addition, we do not find an absorption threshold as it is observed with semiconductors. Immediately, as soon as light is shed on the alloy, its atoms absorb the photons falling on it. We record three prominent peaks in the three regions, which we mention from lowest to highest, which are corresponding at the values of 2.5, 6 and 9.8 eV respectively, these values indicate that the compound is opaque. The change in the energy of the incident photons leads to different optical behaviors in this material. This result is close to work [22].

3.2.1 Optical conductivity

It is among the physical properties that relate current density to the electric field of frequency, as it is closely related to the dielectric constant known by the following equation:

$$\sigma(w) = \frac{J(w)}{E(w)} \quad (2)$$

Where σ is optical conductivity (S/m), J is current density (A/m^2) and E is electric field(N/C).

The photoconductivity values for $FeNi_3$ were calculated with approximations GGA; the results are as shown in Fig.3

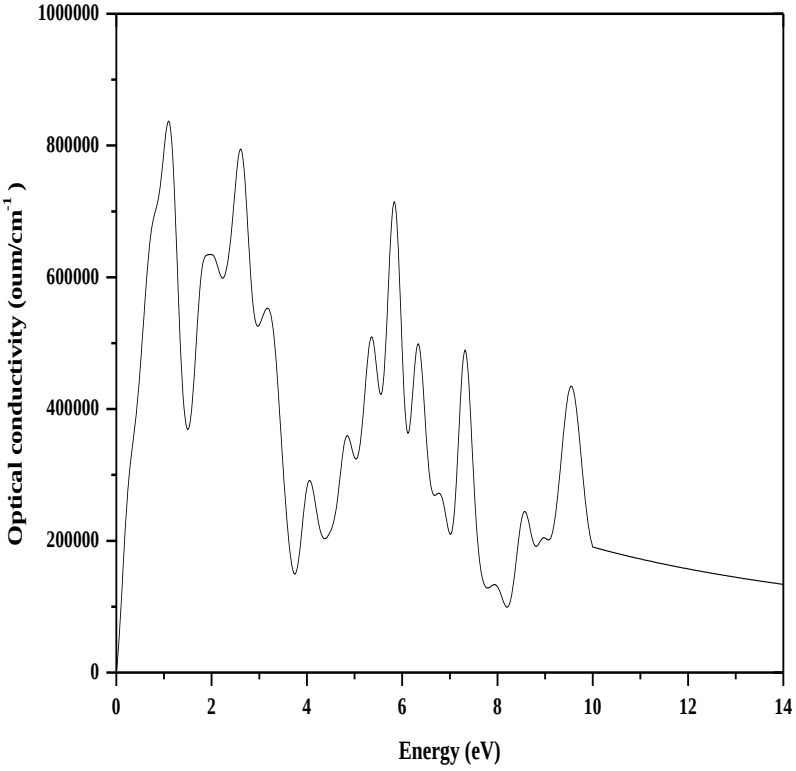

Fig. 3. Optical conductivity of $FeNi_3$ alloy.

Fig.3. represents the photoconductivity changes in terms of the energy of photons falling on the $FeNi_3$ alloy using the GGA approximations; we noticed that the optical conductivity value is directly recorded once the alloy is exposed to photons. It generally records a fluctuation in the optical conductivity values, as it has witnessed an increase with the increase in the energy of the incident photons, and this is during the range energy 0 to 1 eV, which corresponds to infrared radiation. On the other hand, the visible field witnesses higher values in optical conductivity compared to the ultraviolet field. While at the highest energy values, a severe decrease in the optical conductivity is seen.

We conclude from the analysis of the absorption and optical conductivity curves that the $FeNi_3$ alloy has a maximum absorption value that allows its use in optoelectronics and optical energy compounds in the infrared and visible range.

3.2.2. Reflectivity coefficient

The reflectivity (R) can be expressed by the equation:

$$R = [(n_0 - 1)^2 + \frac{K_0^2}{(n_0+1)^2} + K_0^2] \quad (3)$$

Where R is reflectivity coefficient, n_0 is refractive index and k_0 is extinction coefficient. The reflectivity coefficient values for FeNi3 alloy is shown in Fig. 4.

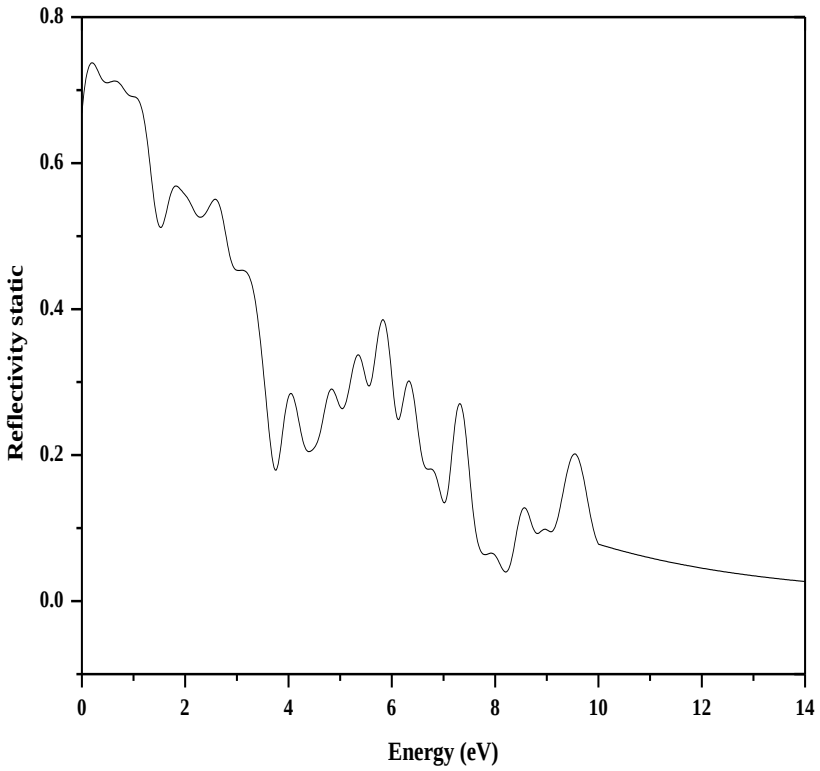

Fig. 4. Reflectivity coefficient of $FeNi_3$ alloy.

Fig.4. represents the changes in the reflectivity coefficient in terms of energy. We notice through the curve that the reflectivity values decrease with the increase in the energy of the incident photons, starting from the value of 0.7 corresponding to the energy of 0 eV. So that this decrease is gradual in the form of oscillations, and the infrared region is characterized by greater values of reflectivity compared to the visible and ultraviolet region. Therefore, we conclude that $FeNi_3$ alloy has good reflectivity in the visible region that makes it used in coatings and optical device applications.

4. CONCLUSION

Based on the calculations made according to density function theory (DFT) and we use the generalized gradient approximation (GGA) according to the scheme described by Perdew-Burke-Ernzerhof (PBE), and using Siesta code. In our current work, we focused on studying the structural and optical properties of $FeNi_3$ alloy. Our calculated lattice constant for $FeNi_3$ alloy agrees well with previously available theoretical and experimental results. The absorption coefficient, reflectivity coefficient and optical conductivity results indicate that $FeNi_3$ alloy is a good candidate for applications in the visible and infrared range.

REFERENCES

1. P. Jing, M. Liu, Y. Pu, Y. Cui, Z. Wang, J. Wang, Q. Liu, *Sci. Rep.* **6**, 37701 (2016).https://doi.org/10.1038/srep37701

2. G. Nahrwold, J. M. Scholtyssek, S.Motl-Ziegler, O. Albrecht, U. Merkt, G. Meier, *J. Appl. Phys.* **108**, 013907 (2010).https://doi.org/10.1063/1.3431384
3. H. Chen, C. Xu, G. Zhao, Y. Liu, *Mater. Lett.* **91**, 75 (2013).https://doi.org/10.1016/j.matlet.2012.09.040
4. E.F. Wasserman,in: Ferromagnetic Materials North-Holland Amsterdam **237**, 322 (1990).
5. A.V. Ruban, S. Khmelevskyi, P. Mohnand, B. Johansson, *Phys. Rev. B***76**, 014420 (2007).https://doi.org/10.1103/PhysRevB.75.054402
6. B. Dutta, S. Ghosh*Intermetallics*, **8**, 1143 (2010).https://doi.org/10.1016/j.intermet.2010.02.052
7. Y. Benkrima, D. Belfennache, R.Yekhlef, M. E. Soudanic , A. Souigat, Y. Achour, *East. Eur.J. Phys.* **2**, 150 (2023) https://doi.org/10.26565/2312-4334-2023-2-14
8. Y. Achour, Y. Benkrima, I. Lefkaier, D. Belfennache, *J. Nano- Electron. Phys.* **15(1).** 01018(5pp) (2023). DOI: 10.21272/jnep.15(1).01018
9. F.H. Rawwagah, A.F. Lehlooh, S.H. Mahmood, S. Mahmoud, A.R. El-Ali, M.R. Said, I. Odeh, I. Abu-aljarayesh, *Jordan. J. Phys*, **5**, 9 (2012).https://doi.org/10.48550/arXiv.1711.03051
10. H. Ullrich, J. Hesse, *J. Magn, Mater*, **5,** 45315 (1984).
11. P.J. Brown, K.U. Neumann, K.R.A. Ziebeck, *J. Phys.Cond. Matt.***13**, 1563 (2001). https://doi.org/10.1088/0953-8984/13/7/317
12. X. Jiang, G.E. Ice, C.J. Sparks, L. Robertson, P. Zschack, *Phys. Rev. B*, **54**, 3211 (1996). https://doi.org/10.1103/PhysRevB.54.3211
13. G. Cacciamani, A. Dinsdale, M. Palumbo, A. Pasturel, *Intermetallics*, **18**, 1148 (2010).https://doi.org/10.1016/j.intermet.2010.02.026
14. N.Y. Pandya, A.D. Mevada, P.N. Gajjar, *Comput. Mater. Sci*, **123**, 287 (2016).https://doi.org/10.1016/j.commatsci.2016.07.001
15. M.J. Wang, G.W. Zhang, H. Xu, J. Phys. Conf. Ser, **1507**, 082026 (2020).https://doi.org/10.1088/1742-6596/1507/8/082026
16. Y. Achour, Y. Benkrima, I. Lefkaier, D. Belfennache, *J. Nano- Electron. Phys.* **15(1).** 01018(5pp) (2023).https://doi.org/10.21272/jnep.15(1).01018
17. P. Ordejón, E. Artacho, J.M. Soler, *Phys. Rev. B.***53**, 10441 (1996).https://doi.org/10.1103/physrevb.53.r10441
18. J.M. Soler, E. Artacho, J.D. Gale, A. Garcıa, J. Junquera, P. Ordejon, D. Sanchez-Portal, *J. Phys. Condens. Matter.* **14**, 2745 (2002).https://doi.org/10.1088/0953-8984/14/11/302
19. Q. Chang, Y. Sun, B.K. Wang, S. Tay, H. Li, Y.B. Huang Zhang, *J. Phys. Chem. B.***106**, 10701 (2002).https://doi.org/10.1021/jp025868l
20. Le. Tuan, V. Tran. Hoan, Nguyen V.Duy, *Comput. Mater.Sci,***180**, 109715 (2020). https://doi.org/10.1016/j.commatsci.2020.109715
21. K.Chen, S. Kim, R. Rajendiran, K. Prabakar, G. Li, Z.Shi, C. Jeong, J. Kang, O. L.Li, *J. Coll. Inter Sci,***582**, 977 (2021). https://doi.org/10.1016/j.jcis.2020.08.101
22. B. Nourozia, A. Aminian, N. Fili, Y. Zangeneh, A. Boochani, P. Darabi, *Results Phys*, **12**, 2038 (2019).https://doi.org/10.1016/j.rinp.2019.02.054